Numerical investigations of resistive wall wake potentials

F. Yaman✉

The aim of this Letter is to examine and identify longitudinal resistive wall wake potential behaviours of medium-β long bunches and ultra-relativistic short bunches using different beam and pipe properties for particle accelerator applications. The lack of detailed analysis in current literature for the chosen set of parameters ignites this work. Since computations of wake potentials for the considered beam parameters by particle-in-cell codes are extremely difficult the author uses an analytical approach. Numerical integrations are evaluated for large domains with fine discretisations. The author observes that conductivity of beam pipe has a larger impact on medium-β long bunches, variation of beam velocity effects wakes of short bunches more significantly, beam radii changes may have a contribution to instability for low energy short bunches. Interesting numerical results are presented and their physical explanations are discussed in this Letter.

Introduction: When a bunch of charged particles passes through accelerator structures wake electromagnetic fields occur due to cross-section change, surface resistivity variations of the beam pipe or existence of an electron cloud formation inside the beam pipe which may result in emittance growth, trajectory change and beam loss for the trailing particles [1–5]. Therefore, accurate determination of the wakefields which can be quantified via wake potentials is a critical issue to reach high energies for the new particle physics experiments.

Mathematically, longitudinal wake potentials can be calculated via the convolution integral of wake functions $G_\parallel$ with the charge distribution of the beam

$$W(\tau) = \int_0^\infty \mathrm{d}t\, G_\parallel(t)\,\lambda(\tau - t), \tag{1}$$

where λ is the normalised line density and τ is a time-dependent parameter, [1]. Wake function is actually the normalised integral of the electromagnetic force due to fields excited by a point charge or delta function distribution, and therefore wake function can be considered as Green's function of the structure [1]. Accordingly, the longitudinal wake function is defined as

$$G_\parallel(\boldsymbol{r}_\mathrm{e}, \boldsymbol{r}_\mathrm{t}, t) = -\frac{1}{q}\int_{-\infty}^{\infty} \mathrm{d}z\, E_z(\boldsymbol{r}_\mathrm{e}, \boldsymbol{r}_\mathrm{t}, z, t = (z+s)/v), \tag{2}$$

where E_z is the longitudinal component of the electric field, q is the charge of exciting point-like particle, s is the distance between the source and following test charge, $\boldsymbol{v}$ is the speed of source and test charges, $(\boldsymbol{r}_\mathrm{e}, \boldsymbol{r}_\mathrm{t})$ are transverse offsets of the exciting and the test particles from the z-axis, respectively. The Fourier transform of the wake function which is called the coupling impedance can be expressed as

$$Z_\parallel(\boldsymbol{r}_\mathrm{e}, \omega) = -\frac{1}{\hat{I}}\int_{-\infty}^{\infty} \mathrm{d}z\, \hat{E}_z(\boldsymbol{r}_\mathrm{e}, z)\, \mathrm{e}^{-\mathrm{i}\omega z/v}, \tag{3}$$

in terms of the frequency domain representations of the longitudinal electric field component $\hat{E}_z$, and the current $\hat{I}$, for the angular frequency ω. Corresponding transverse wake functions and coupling impedances can be obtained from the longitudinal wake functions and impedances by applying the Panofsky–Wenzel theorem.

Coupling impedances consist of the space charge and resistive wall impedance components. In this study, we focus on the numerical calculations and the physical interpretations of wake potentials due to resistive wall impedances and omit the effect of space charge which is related to bunch properties. For the longitudinal monopole resistive wall impedances $Z_\parallel^{rw}$, Al-khateeb *et al.* model [6] is employed since it is applicable for both non-relativistic and ultra-relativistic long/short bunches. Furthermore, Laslett *et al.* [7], Gluckstern [8], Zimmermann and Oide [9], Mounet [10], Macridin *et al.* [11] are important contributions on the impedance calculations for non-ultra-relativistic cases. In [12], Zannini *et al.* presented the limitations of longitudinal and transverse impedances via CST 3D simulations in the non-relativistic regime which could be an indication of the significance of the current work. Principally, the particle-in-cell codes have difficulties from computational and accuracy points of view in the evaluations of wake potentials for short bunches such that one can suggest the studies [13, 14], for different treatments. Within this framework, we employ an analytical model to compute wake potentials for the sake of the accuracy and to expand the limitations of the alternative approaches.

The structure of the paper is as follows, the longitudinal resistive wall impedance problem, the analytical impedance model for the solution, and wake calculations are introduced in the next section. The following part is focused on the wake potential observations and their physical interpretations in the proposed parameter scope. In the final section conclusions and concluding remarks are presented.

Impedance model and wake potential calculations: In Al-khateeb *et al.* impedance model [6], the non-homogeneous wave equation

$$\begin{aligned}\Delta\boldsymbol{E} - \frac{1}{c^2}\frac{\partial^2\boldsymbol{E}}{\partial t^2} &= \mu_0\frac{\partial\boldsymbol{J}}{\partial t} + \frac{\nabla\rho_c}{\epsilon_0},\\ \Delta\boldsymbol{B} - \frac{1}{c^2}\frac{\partial^2\boldsymbol{B}}{\partial t^2} &= -\mu_0\nabla\times\boldsymbol{J}.\end{aligned} \tag{4}$$

is solved for the given charge $\rho_c = \widetilde{\rho_c}(r, \theta)\delta(z - vt)$ and the current densities $\boldsymbol{J} = \rho_c\,\boldsymbol{v}$ for the electric $\boldsymbol{E}$, and magnetic $\boldsymbol{B}$, fields in a smooth circular cylindrical accelerator ring with a circumference L. Here we note that infinitesimally thin disk beam with the radius a, travels at a constant longitudinal velocity $\boldsymbol{v}$ at the centre of the beam pipe whose radius is denoted by b. Accordingly, the resistive wall impedance at $r = a$ can be obtained as

$$\begin{aligned}Z_\parallel^{rw}(a, \omega) = {} & \frac{2LI_1^2(k_r\,a)}{\pi a^2\epsilon_0\omega}\\ & \times\left[\frac{(\beta\gamma Z_m/c\mu_0)K_1(k_r\,b) + \mathrm{i}\,K_0(k_r b)}{I_0(k_r b) + \mathrm{i}(\beta\gamma Z_m/c\mu_0)I_1(k_r b)} - \mathrm{i}\frac{K_0(k_r b)}{I_0(k_r b)}\right],\end{aligned} \tag{5}$$

where $Z_m = (1+i)/\sigma\delta_s$ is the surface impedance on the beam pipe walls, σ is the conductivity, δ_s is the skin depth, I_j and K_j are the jth order modified Bessel functions, $k_r = \omega/\gamma\beta c$ and $\beta = v/c$, c is the speed of light, γ is the Lorentz factor, ϵ_0, μ_0 are the free space permittivity and permeability, respectively.

Longitudinal wake function $G_\parallel^{rw}$, which can be considered as the response of a structure to an infinitely short bunch is calculated via the Fourier integral,

$$G_\parallel^{rw}(z) = \frac{1}{2\pi}\int_{-\infty}^{\infty} \mathrm{d}\omega\, Z_\parallel^{rw}(\omega)\, \mathrm{e}^{-\mathrm{j}\frac{\omega}{\beta c}z}. \tag{6}$$

By considering the analogy with Green's functions, they can be employed in the convolution with finite length Gaussian bunches for the wake potential calculations,

$$W(\tau) = \frac{1}{\sqrt{2\pi}\sigma_z}\int_0^\infty \mathrm{d}t\, G_\parallel^{rw}(t)\exp\left[-\frac{(\tau - t)^2}{2\sigma_z^2}\right]. \tag{7}$$

It is worth to mention that the accurate numerical computations for the wake potentials the main difficulty appears in the numerical computation of the convolution integral for very short wake functions and meter length bunches.

Numerical results and physical interpretations: Parameter scope of the numerical examples is decided by considering kinetic energy of the bunches vary in the range of $E_k = \{\infty, 145.35, 4.73\}$ MeV which correspond to $\beta = \{\simeq 1, 0.5, 0.1\}$. Furthermore, bunches contain $N_p = 6.2\times 10^{10}$ protons with the length of $\sigma_z = \{1\times 10^{-4}, 1\}m$ and radius of $a = \{\simeq 0, 0.5\}$ cm are used in the numerical examples. The conductivity of the beam pipe is selected from a set of values $\sigma = \{100, 1\times 10^4, 1\times 10^6\}$ S/m and pipe radius is chosen from $b = \{1, 5, 10\}$ cm. The verification of the code is presented in [15] by comparing CST-Wak Solver, 2D-ECHOz and different analytical approaches.

In the numerical results section the effects of different conductivities $\sigma = \{100, 1\times 10^4, 1\times 10^6\}$ S/m and different beam pipe radii $b = \{1, 5, 10\}$ cm on wake potentials are illustrated in Figs. 1 and 2, respectively. Afterwards, contributions of beam parameters such as velocity and radius to the wake potentials are presented in Fig. 3 and in Fig. 4. We define $\beta = 0.5$ as medium-β, $\sigma_z = 1$ m as a long bunch, $\beta \simeq 1$ as an ultra-relativistic beam and $\sigma_z = 100\,\mu$m as a short bunch in the investigations. Note that λ_N, which appears in the following plots indicates the normalised beam charge density.

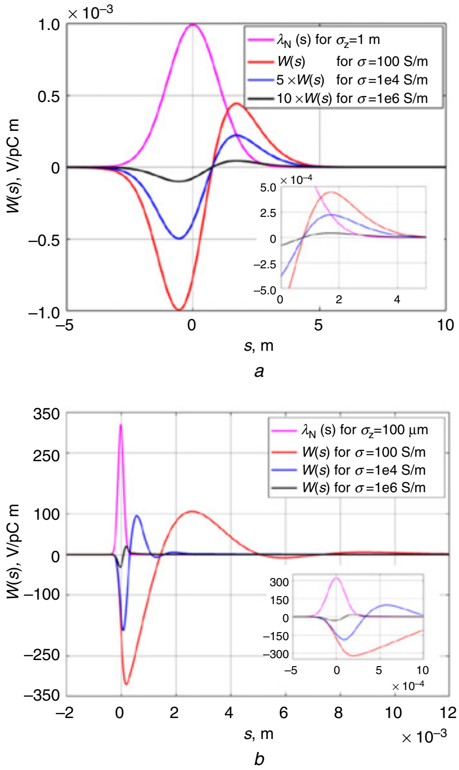

Fig. 1 *Wake potentials of medium-β long and ultra-relativistic short bunches for different conductivities*

a $\beta = 0.5$, $a = 0.5\,\text{cm}$, $b = 1\,\text{cm}$
b $\beta \simeq 1$, $a = 0.5\,\text{cm}$, $b = 1\,\text{cm}$

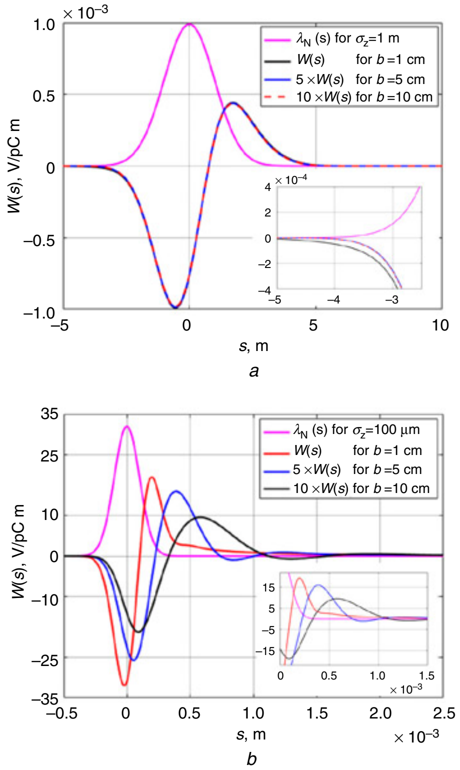

Fig. 2 *Wake potentials of medium-β long and ultra-relativistic short bunches for different beam pipe radii*

a $\beta = 0.5$, $a = 0.5\,\text{cm}$, $\sigma = 1 \times 10^6\,\text{S/m}$
b $\beta \simeq 1$, $a = 0.5\,\text{cm}$, $\sigma = 1 \times 10^6\,\text{S/m}$

According to Fig. 1*a*, wake potential profiles (zero crossings and peak positions) are not affected by the variations of σ, but wake values decrease at least by factor 10 when the conductivity of the beam pipe material increases by four orders of magnitude for the medium-β long bunches. Furthermore wakes reach their peaks in front of the centre of the proton bunches due to slower beam velocities as compared to the propagation of electromagnetic fields, however this behaviour changes for the ultra-relativistic short bunches as it is illustrated in Fig. 1*b*. Another major difference appears in the high wake values for the short bunches, e.g. $\simeq 5$ orders of magnitude larger than the medium-β long bunches. In addition to this we observe from Fig. 1*b* that variations of conductivity values have less impact on the wake magnitude changes for short bunches, i.e. all the wakes could be illustrated on a single plot without rescalings for $\sigma = 1 \times 10^4\,\text{S/m}$ and $\sigma = 1 \times 10^6\,\text{S/m}$ cases, but the oscillations behind the short beam exist for a longer time duration for the smaller σ values, e.g. for $\sigma = 100\,\text{S/m}$.

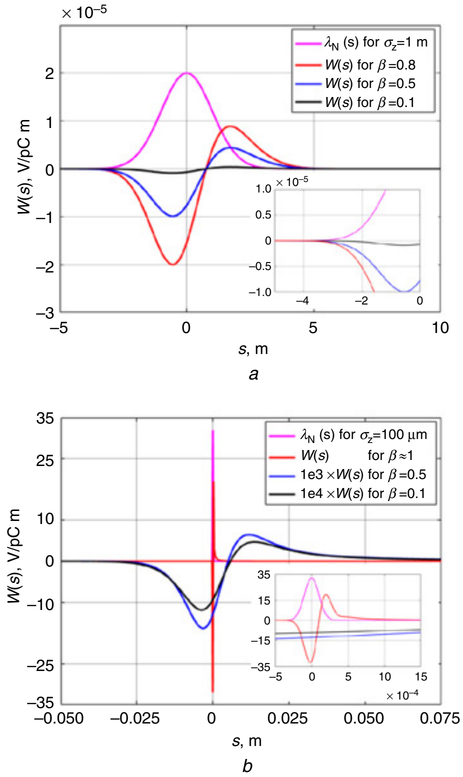

Fig. 3 *Wake potentials of medium-β long and ultra-relativistic short bunches for different velocities*

a $a = 0.5\,\text{cm}$, $b = 1\,\text{cm}$, $\sigma = 1 \times 10^6\,\text{S/m}$
b $a = 0.5\,\text{cm}$, $b = 1\,\text{cm}$, $\sigma = 1 \times 10^6\,\text{S/m}$

Conductivity variations have a more significant impact on the magnitude of the wake potentials for medium-β long bunches as compared to the ultra-relativistic short bunches. Long bunches excite electromagnetic waves with low-frequency components which can penetrate into the beam pipe deeper than high-frequency components. As a result of the loss mechanism in the beam pipe, conductivity changes cause higher variations in the wake potential amplitudes for long bunch applications. Since high-frequency electromagnetic components generated by ultra-relativistic short bunches are mostly reflected from the beam pipe walls, conductivity has a weaker effect on wake potential magnitudes as compared to the longer bunches.

From Fig. 2*a* an approximately linear behaviour for medium-β long bunches with respect to beam pipe radii can be noticed. Here the factor for scaling the beam pipe radii can be employed to scale the resultant wake potential in order to obtain a good match to the wake for $b = 1\,\text{cm}$. The subplot which focuses/zooms on the difference of the wakes for different beam pipe radii, and emphasises the approximate linearity, is also presented inside of Fig. 2*a*. In Fig. 2*b* the magnitude of the wakes decreases with the increase in the beam pipe radius as expected but at the same time, the initial wake oscillation shifts to behind of the centre of bunch. This particular case is not observed for a $\sigma_z = 1\,\text{m}$ bunch, see Fig. 2*a*. Additionally wake potential oscillations are quickly vanishing in Fig. 2*b* as compared to Fig. 1*b* (see the values of the *s*-axis for both figures) which means that the effect of conductivity changes on electromagnetic fields lasts longer as compared to beam pipe radii variations for $\sigma_z = 100\,\mu\text{m}$ bunches. On the contrary, the wakes for medium-β long bunches disappear from the same distance behind the centre of bunch, see Figs. 1*a* and 2*a*. Fig. 3 is devoted to compare values of wake magnitudes and to express variations of wakes for long/short bunches at different velocities. As an obvious result from the figure the larger wake potentials occur for two different bunch lengths when the beam accelerates, and this effect can be observed more clearly on a $\sigma_z = 100\,\mu\text{m}$ bunch, (see the scaling factors in Fig. 3*b*). Furthermore for the ultra-relativistic case the wake distribution is confined in a small area, whereas wakes of the slower beams decay slowly. Additionally, when shorter bunches travel at medium/low velocities, e.g. $\beta \leq 0.5$, wakefields occur at larger distances(normalised to the bunch length) in front of the bunch centre as compared to longer bunches at similar velocities.

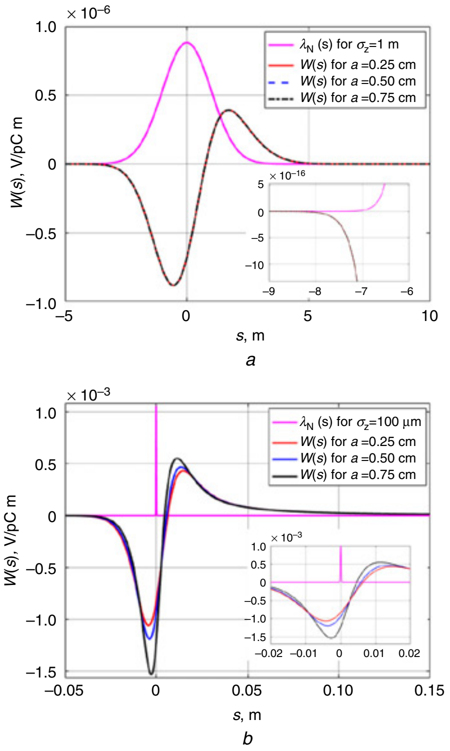

Fig. 4 *Wake potentials of medium-β long and ultra-relativistic short bunches for different beam radii*

a $\beta = 0.1$, $b = 1\,\text{cm}$, $\sigma = 1 \times 10^6\,\text{S/m}$
b $\beta = 0.1$, $b = 1\,\text{cm}$, $\sigma = 1 \times 10^6\,\text{S/m}$

For long bunches, wake potentials with respect to the β of the beam do not vary much, whereas for very short bunches, wake potentials change a lot with the increase of beam velocity. Assume two bunches at the same energy but one is long($\simeq [m]$ range) and the other is short ($\simeq [\mu\text{m}]$ range). Frequency spectrum of the electromagnetic waves generated by two bunches can be calculated via the Fourier transform. In this case, it can be observed that the electromagnetic waves generated by the short bunches have higher frequency components than the waves excited by the longer bunches. Therefore according to the skin depth mechanism, it is expected to be that the wake potentials are affected more from β increase for the short bunches.

In Fig. 4, the effect of beam radii on wakes is investigated. Mathematically, beam radii values contribute to the wake potential results by a factor $I_1^2(k_r a)/a^2$ which can be seen from the Al-khateeb *et al.* impedance model, given in (5). However, the effect of beam radii is observed only for the short bunches $\sigma_z = 100\,\mu\text{m}$ at low velocities $\beta = 0.1$ even though the same parameters are tested for long bunches $\sigma_z = 1\,\text{m}$, (Figs. 4*a* and *b*. Furthermore, with a conductivity $\sigma = 100\,\text{S/m}$, the beam radii change do not have an influence on wake potentials neither for $\sigma_z = 100\,\mu\text{m}$ bunches at $\beta \simeq 1$ nor $\sigma_z = 1\,\text{m}$ at $\beta = 0.8$ in our numerical experiments.

Contribution of the larger beam radius to the wake potentials appears only for $\beta = 0.1$, $\sigma_z = 100\,\mu\text{m}$ bunches. This is related to the increase of the coupling impedance between beam and beam pipe for larger beam radii. Since the wake potentials are larger for shorter bunches this effect becomes noticeable. However, beam radius impact is not observed for ultra-relativistic short bunches. In the ultra-relativistic limit, the fields created by the charges at different transversal positions of the bunch cancel each other out and do not bring contribution to the longitudinal electric field.

Conclusions: According to our observations, in most cases wake potential behaviours (zero crossings and peak positions) of long bunches do not vary w.r.t. conductivity, beam pipe radius, beam radius and velocity. However, this is not the case for very short bunches. Due to skin effect, high-frequency components of the electromagnetic waves generated by short bunches penetrate less into the metallic pipe walls. Therefore these components, which carry higher energy in the electromagnetic spectrum, are confined in the hollow region of the beam pipe. Thus wake potential distribution on the longitudinal axis becomes more sensitive to parameter changes. As a remedy, one can increase the beam pipe radius but this update extends the effect of wakes behind the beam in a longer time. In this case, the sequential bunch spacings should be increased which leads to a decrease of bunch loadings in the accelerator ring. The inverse relation between pipe radii and wake potential is approximately linear for medium-β, $\sigma_z = 1\,\text{m}$ bunches. Furthermore, it is observed that changing the pipe conductivity can distort the wake potential profiles of ultra-relativistic short bunches which is not the case for medium-β long bunches. The effect of beam radius is seen only for $\sigma_z = 100\,\mu\text{m}$ for low-beta $\beta = 0.1$ values.

Acknowledgments: The author thanks Dr Fritz Caspers (CERN) for constructive criticism of the manuscript.

Submitted: *21 August 2019* E-first: *11 November 2019*
doi: 10.1049/el.2019.2830
One or more of the Figures in this Letter are available in colour online.

F. Yaman (*Electrical and Electronics Engineering Department, Izmir Institute of Technology, Urla, Izmir 35430, Turkey*)

✉ E-mail: fatihyaman@iyte.edu.tr

References

1 Zotter, B.W., and Kheifets, S.A.: 'Impedances and wakes in high energy particle accelerators' (World Scientific, Singapore, 1998)
2 Chao, A.W.: 'Physics of collective beam instabilities in high energy accelerators' (Wiley, New York, NY, USA, 1993)
3 Ng, K.Y.: 'Physics of intensity dependent beam instabilities' (World Scientific, Singapore, 2006)
4 Weiland, T.: 'Transverse beam cavity interaction part I: short range forces', *Nucl. Instrum. Methods Phys. Res.*, 1983, **212**, (1–3), pp. 13–21
5 Boine-Frankenheim, O., Gjonaj, E., Petrov, F., *et al.*: 'Energy loss and longitudinal wakefield of relativistic short proton bunches in electron clouds', *Phys. Rev. Spec. Top., Accel. Beams*, 2012, **15**, (5), p. 054402
6 Al-Khateeb, A.M., Boine-Frankenheim, O., Hofmann, I., *et al.*: 'Analytical calculation of the longitudinal space charge and resistive wall impedances in a smooth cylindrical pipe', *Phys. Rev. E*, 2001, **63**, (2), p. 026503
7 Laslett, L.J., Neil, V.K., and Sessler, A.M.: 'Transverse resistive instabilities of intense coasting beams in particle accelerators', *Rev. Sci. Instrum.*, 1965, **36**, (4), pp. 436–448
8 Gluckstern, R.L.: 'Analytic methods for calculating coupling impedances', vol. 11 (CERN, Geneva, Switzerland, 2000)
9 Zimmermann, F., and Oide, K.: 'Resistive-wall wake and impedance for nonultrarelativistic beams', *Phys. Rev. Spec. Top., Accel. Beams*, 2004, **7**, (4), p. 044201
10 Mounet, N.: 'The LHC transverse coupled-bunch instability', PhD Thesis, Ecole Polytechnique Federale de Lausanne, 2012
11 Macridin, A., Spentzouris, P., and Amundson, J.: 'Impedances and wake functions for non-ultrarelativistic beams in circular chambers', Technical Report, Fermi National Accelerator Lab., Batavia, IL, USA, 2012
12 Zannini, C., Rumolo, G., and Rijoff, T.: 'Electromagnetic simulations for non-ultrarelativistic beams and applications to the CERN low energy machines', 5th International Particle Accelerator Conference, Dresden, Germany, June 2014, pp. 1–4
13 Zagorodnov, I., Schuhmann, R., and Weiland, T.: 'Long-time numerical computation of electromagnetic fields in the vicinity of a relativistic source', *J. Comput. Phys.*, 2003, **191**, (2), pp. 525–541
14 Dohlus, M., and Zagorodnov, I.: 'Explicit TE/TM scheme for particle beam simulations', *J. Comput. Phys.*, 2009, **228**, (8), pp. 2822–2833
15 Yaman, F.: 'Quantification of resistive wall instability for particle accelerator machines', *Turk. J. Electr. Eng. Comput. Sci.*, 2019, pp. 1–12, doi:10.3906/elk-1903-194